RSC Advances

ROYAL SOCIETY OF CHEMISTRY

www.rsc.org/advances

Selective photodegradation of 2-mercaptobenzothiazole by the novel imprinted $CoFe_2O_4$/MWCNTs photocatalyst

Ziyang Lu,[a,b] Ming He,[b] Lili Yang,[b] Zhongfei Ma,[a] Li Yang,[b] Dandan Wang,[b] Yongsheng Yan,[*,b] Weidong Shi,[b] Yang Liu[b] and Zhoufa Hua[b]

Novel imprinted $CoFe_2O_4$/MWCNTs photocatalyst was prepared through combination of hydrothermal method and suspension polymerization based on 2-mercaptobenzothiazole (MBT) as the molecular template, pyrrole as the imprinted functional monomer and conductive polymerizable monomer, $CoFe_2O_4$/MWCNTs as the matrix material. The results indicated that the surface imprinted layer was successfully coated on the surface of $CoFe_2O_4$/MWCNTs and polypyrrole (PPy) was formed and existed in the surface imprinted layer, the magnetic saturation value of novel imprinted $CoFe_2O_4$/MWCNTs photocatalyst was 19 emu/g. Moreover, compared with other photocatalysts, novel imprinted $CoFe_2O_4$/MWCNTs photocatalyst not only had high photocatalytic efficiency (57.09 %), but also possessed the strong ability to selective recognition and photodegradation of MBT (The coefficients of selectivity of novel imprinted $CoFe_2O_4$/MWCNTs photocatalyst relative to $CoFe_2O_4$/MWCNTs and non-imprinted $CoFe_2O_4$/MWCNTs photocatalyst was 3.37 and 3.28, respectively). In addition, in the process of photodegradation reaction, h^+ and $\cdot OH$ were the main oxidative species, $\cdot O_2^-$ played a very small role.

a. School of the Environment and Safety Engineering, Jiangsu University, Jiangsu, Zhenjiang 212013, PR China.
b. School of Chemistry & Chemical Engineering, Jiangsu University, Jiangsu, Zhenjiang 212013, PR China.
E-mail: luziyang126@126.com.

Introduction

2-mercaptobenzothiazole (MBT) is an odorous, toxic and poorly biodegradable chemical with a –SH group and isolated electron pairs.[1] It is normally used as a corrosion inhibitor, antifungal drug, pesticides fungicide and vulcanization accelerator of rubber. MBT has been detected in wastewater effluents, river water, sewage treatment works and surface water.[2, 3] A low concentration of MBT might inhibit the biodegradation of other organics and the nitrification of wastewater. Moreover, MBT has been shown to induce tumors, to be allergenic, to be toxic to aquatic organisms, to hamper wastewater treatment.[4] Therefore, it is necessary to develop methods to effectively remove MBT in the aquatic environment.

Photocatalytic technology has received much attention to their application potential for complete mineralization of many toxic and non-biodegradable organics.[5-7] For example, Habibi et al. investigated the photocatalytic oxidation of five kinds of mercaptans and found that these mercaptans could be almost completely mineralized to carbon dioxide and sulfate ion.[3] However, common photocatalysts are difficult to recycle. Therefore, spinel ferrites (MFe_2O_4, M=metal cation)[8] is introduced because it can be easily collected by a magnet and maintains a very high recycling rate. Meanwhile, MFe_2O_4 has a relatively narrow band gap, which can be excited under the light irradiation. Cobalt ferrite ($CoFe_2O_4$), with unique physical, electric and magnetic properties,[9] has been utilized as photocatalyst for the degradation of various environmental pollutants.[10, 11] In recent years, the photocatalytic activity of $CoFe_2O_4$ has been improved through coupling with carbonaceous materials,[8] such as Multi-walled carbon nanotubes (MWCNTs).[12, 13] MWCNTs, as a typical kind of carbonaceous materials, have attracted great interest for their large

specific surface area, high mechanical strength, thermal stability, good compatibility and remarkable electrochemical properties.[14, 15] $CoFe_2O_4$/MWCNTs nanocomposites have been synthesized through solvothermal method, electrospinning, in situ high-temperature hydrolysis, chemical vapor deposition method and so on.[16]

Nevertheless, common photocatalysts have very poor selectivity which cannot differentiate high toxic target pollutant from other low toxic organic pollutants.[17] Recently, a new strategy of enhancing the selectivity is surface imprinting technique which is a convenient method for preparing polymer with the ability of recognizing and specifically binding the target molecule.[18-22] However, the introduction of surface-imprinted layer obviously decreases the photocatalytic efficiency because the surface-imprinted layer covers the active sites of $CoFe_2O_4$.[23]

To improve the photocatalytic activity, conductive polymer is introduced in the synthesis of imprinted photocatalyst.[24] In our work, pyrrole is used not only as the imprinted functional monomer, but also as the conductive polymerizable monomer, namely, the surface imprinted layer not only contains the imprinted polymer, but also contains Polypyrrole (PPy). PPy is one of the most commonly investigated conducting polymers owing to its non-toxic nature, environmental stability, low cost and ease to synthesize.[25] When the composite photocatalyst is irradiated by the visible light, the photo-generated electrons (e^-) and photo-induced holes (h^+) will generate in PPy and $CoFe_2O_4$, this combination between PPy and $CoFe_2O_4$ enhance the transfer of e^- and h^+. Thus more and more e^-/h^+ form and trigger the formation of very reactive radicals super-oxide radical ion ($O_2\cdot^-$) and hydroxyl radical ($\cdot OH$), which are responsible for the photodegradation of MBT. Therefore, the introduction of PPy can greatly enhance the photodegradation activity.

In addition, considering the formation of recognition sites, avoiding bead agglomeration and

simplifying laborious procedures, suspension polymerization is one of the best methods to be adopted.[26] As far as we know, no report has studied this kind of novel imprinted $CoFe_2O_4$/MWCNTs photocatalyst.

In this work, by using pyrrole as the imprinted functional monomer and conductive polymerizable monomer, MBT as the molecular template, $CoFe_2O_4$/MWCNTs as the matrix material, novel imprinted $CoFe_2O_4$/MWCNTs photocatalyst was prepared by combining hydrothermal method with suspension polymerization. The as-prepared photocatalyst was further characterized by X-ray diffraction (XRD), inductively coupled plasma optical emission spectrometry (ICP-OES), fourier transform infrared spectra (FT-IR), transmission electron microscope (TEM), N_2 adsorption-desorption analysis with the Brunauer-Emmett-Teller (BET) method, UV-visible diffuse reflectance spectra (UV-vis DRS) and vibrating sample magnetometer (VSM). Moreover, a series of influence factors was investigated (such as the concentration of pyrrole, the concentration of MBT). Finally, the photocatalytic reaction (containing adsorption capacity, degradation rate, selectivity and mechanism) of novel imprinted $CoFe_2O_4$/MWCNTs photocatalyst was also investigated.

Experimental section

Materials

Multi-walled carbon nanotubes (MWCNTs, 50 nm in diameter and 10-20 μm in length) with special surface area of more than 40 m^2/g were provided by Beijing DK nano technology Co. Ltd. 2-mercaptobenzothiazole (MBT, $C_7H_5NS_2$, 98%) and trimethylolpropane trimethacrylate (TRIM, 80%) were purchased by Aladdin Chemistry Co. Ltd. 2, 2'-Azobis-(2,4-dimethylvaleronitrile)

(ABVN, 97%) was purchased by J&K Scientific Ltd. Iron (III) nitrate nonahydrate ($Fe(NO_3)_3 \cdot 9H_2O$), cobalt nitrate hexahydrate ($Co(NO_3)_2 \cdot 6H_2O$), polyethylene glycol 4000 (PEG 4000, CP), pyrrole (CP), trichloromethane ($CHCl_3$, AR), sodium hydroxide (NaOH, AR), methanol (CH_3OH, AR) and anhydrous ethanol (C_2H_5OH, AR) were all purchased from Sinopharm Chemical Reagent Co. Ltd. Sulfuric acid (H_2SO_4, 95%-98%), nitric acid (HNO_3, 65%-68%), hydrogen peroxide (H_2O_2, 30%) and hydrochloric acid (HCl, 36%-38%) were used as received. Deionized and doubly distilled water (DDW) was used throughout this work.

Preparation process

Preparation of $CoFe_2O_4$/MWCNTs photocatalyst

The purification of the MWCNTs was treated as follows: 0.5 g MWCNTs was added into a mixture (contained 15 mL nitric acid and 45 mL sulfuric acid) with mechanical agitation for 6 h at 60 ℃. Afterwards, the purified MWCNTs was washed with DDW to neutral and dried under vacuum overnight at 40 ℃ for further use.

$CoFe_2O_4$/MWCNTs were prepared through hydrothermal synthesis.[27] 0.291g $Co(NO_3)_2 \cdot 6H_2O$ and 0.808g $Fe(NO_3)_3 \cdot 9H_2O$ were dissolved in 30 mL DDW by ultrasonication at room temperature for 10 min. Afterwards, 60 mg purified MWCNTs was added into above solution by ultrasonication at room temperature for another 10 min. After 4.5 g NaOH was added, the mixture was vigorously stirred for 30 min and transferred into a 50 mL teflon-lined stainless steel autoclave. The autoclave was sealed and maintained at 180 ℃ for 12 h. The reaction could be explained by the following equation: $Co^{2+} + 2Fe^{3+} + 8OH^- \rightarrow CoFe_2O_4 + 8H_2O$. The black products were collected by a magnet and washed with DDW and anhydrous ethanol for several times until there were no nitrate ions in the solution. Finally, $CoFe_2O_4$/MWCNTs was sealed and

vacuum dried at 40 ℃ overnight.

Preparation of novel imprinted $CoFe_2O_4$/MWCNTs photocatalyst

The novel imprinted $CoFe_2O_4$/MWCNTs photocatalyst was synthesized through suspension polymerization. The activation of $CoFe_2O_4$/MWCNTs was treated as follows: 1 g $CoFe_2O_4$/MWCNTs, 10 g PEG 4000 was added into 150 mL DDW by ultrasonication at room temperature for 10 min, afterwards, the mixture was transferred to a three-neck flask. PEG 4000 was absorbed on the surface of $CoFe_2O_4$/MWCNTs via Van der Waals force and hydrogen bond. Meanwhile, a certain amount of MBT (1mmol, 2mmol, 3mmol, 4mmol or 5mmol) was dissolved into the organic phase of trichloromethane which contained a certain amount of pyrrole (2mmol, 4mmol, 6mmol, 8mmol or 10mmol), 1 mL TRIM (cross-linker) and 0.3025 g ABVN (initiator). Afterwards, above solution was gradually added into the three-neck flask with mechanical agitation at 40 ℃. Kept on stirring and the polymerization was carried out under nitrogen atmosphere for 24 h. Subsequently, the molecular template (MBT) was removed by adding 150 mL DDW into above solution under the UV light irradiation for 3 h with the magnetic agitation under an air atmosphere. The resulting solid product (Novel imprinted $CoFe_2O_4$/MWCNTs photocatalyst) was washed with DDW and anhydrous ethanol each for several times and vacuum dried at 40 ℃ overnight.

The preparation of non-imprinted $CoFe_2O_4$/MWCNTs photocatalyst was prepared under the same polymerization conditions, but without adding MBT. The preparation of imprinted $CoFe_2O_4$ photocatalyst was also prepared under the same polymerization conditions, but without adding MWCNTs.

Characterization

In this work, X-ray diffraction (XRD) patterns were obtained with a D/max-RA X-ray diffractometer (Rigaku, Japan) equipped with Ni-filtrated Cu Kα radiation (40 kV, 200 mA) to characterize the crystal structure. The 2θ scanning angle range was 20-80° with a step of 0.02°/0.2 s. The transmission electron microscope (TEM) images were examined with JEM-2100 transmission electron microscopy (JEOL, Japan). Inductively coupled plasma optical emission spectrometry (ICP-OES, VISTA-MPX) was designed to analyze chemical composition of photocatalysts, the sample was prepared by wet digestion method. 0.1 g photocatalyst, 4 mL HNO_3, 12 mL HCl and 1 mL H_2O_2 were added in a beaker in order. After the solution had nearly evaporated to dryness, it was cooled to room temperature and dilution with distilled water to 250 mL. Fourier transform infraredspectra (FT-IR) were recorded on a Nicolet Nexus 470 FT-IR (America thermo-electricity Company) with 2 cm^{-1} resolution in the range 400 cm^{-1} - 4000 cm^{-1}, using KBr pellets. UV-vis diffuse reflectance spectra (UV-vis DRS) of photocatalyst powder were obtained for the dry-pressed disk samples using it equipped with the integrated sphere accessory for diffuse reflectance spectra, using $BaSO_4$ as the reflectance sample. Ultraviolet-visible spectrophotometer (UV-2450, Shimadzu, Japan) was used for spectrophotometric determination of mercaptans. Specific surface areas were measured by using a NOVA 2000e analytical system (Quantachrome Co., USA). Magnetic measurements were carried out by using a vibrating sample magnetometer (VSM) (HH-15, Nanjing University).

Adsorption experiment

The adsorption capacity was tested in accordance with the following steps: 0.1 g photocatalyst was added into 50 mL 10 mg/L MBT aqueous solution, the sample analysis was conducted at an interval of 10 min at 303 K. After 30 min in the dark, the photocatalyst was

isolated by a magnet, and the concentration of solution was measured with the UV-vis spectrophotometer 2450 (Shimazu Co., Japan).

Photocatalytic activity experiment

The photocatalytic reaction was conducted in a photocatalytic reactor (Fig. 2) at 303 K and initiated by irradiating with a 500 W xenon lamp (the illumination of xenon lamp could reach 1.8×10^5 lux). The photochemical reaction flask contained 0.1 g photocatalyst and 50 mL 10 mg/L MBT aqueous solution. After the desired time in the dark, the initial concentration was determined. Afterwards, the sample analysis was conducted at an interval of 10 min and the aeration rate was 2 mL/min, after the visible light irradiation for 60 min, isolated by a magnet, the concentration was measured with the UV-vis spectrophotometer 2450.

Selective experiment

The selective photodegradation experiment was also carried in accordance with above photocatalytic activity experiment, but the photochemical reaction flask contained 0.10 g photocatalyst and 50 mL 10 mg/L 1-methylimidazole-2-thiol aqueous solution. The coefficient of selection ($k_{selectivity}$) was calculated by using the following formula.

For novel imprinted $CoFe_2O_4$/MWCNTs photocatalyst:

$$k_{imprinted}=\frac{\text{Dr. (MBT)}}{\text{Dr. (1-methylimidazole-2-thiol)}} \quad (1)$$

For other photocatalysts: $$k_{comparison}=\frac{\text{Dr. (MBT)}}{\text{Dr. (1-methylimidazole-2-thiol)}} \quad (2)$$

$$k_{selectivity}=\frac{k_{imprinted}}{k_{comparison}} \quad (3)$$

Reproducibility of novel imprinted $CoFe_2O_4$/MWCNTs photocatalyst

To further evaluate the stability of the photocatalytic activity, 0.1 g non-imprinted

$CoFe_2O_4$/MWCNTs photocatalyst and 50 mL 10 mg/L MBT aqueous solution were added into the photochemical reaction flask, the reaction was conducted at 303 K and initiated by irradiating with a 500 W xenon lamp (the illumination of xenon lamp could reach 1.8×10^5 lux). After the desired time in the dark and the xenon lamp irradiation for 60 min, the recycled sample was isolated by a magnet and sonicated with anhydrous ethanol for 0.5 h to remove the residual MBT and by-products. Finally, the sample was washed with DDW and dried under vacuum at room temperature. This procedure was repeated five times to confirm the photochemical stability.

Results and discussion

Characterization

XRD patterns of $CoFe_2O_4$/MWCNTs and novel imprinted $CoFe_2O_4$/MWCNTs photocatalyst were shown in Fig. 1. Compared with Fig. 1a, some peaks in Fig. 1b became weakened, which was due to the introduction of surface imprinted layer. As can be seen, the peaks appeared at 2θ values of 30.1°, 35.5°, 43.2°, 53.5°, 57.0° and 62.6° could be indexed to $CoFe_2O_4$, which was corresponding well with the PDF#22-1086 data file. This result showed that the introduction of surface imprinted layer did not change the crystallization performance of $CoFe_2O_4$. Furthermore, no peaks related to pure iron or cobalt phases such as hematite or cobalt oxide were identified, indicating that the thermal treatment did not cause phase segregation.[28] Average crystallite size of $CoFe_2O_4$ was estimated according to Scherrer's equation:

$$d=\frac{0.89\lambda}{\beta\cos\theta} \quad (4)$$

Where d is the average crystallite size (nm), λ is the wavelength of the Cu Kα applied (λ=0.15406 nm) and β is the peak width at half-maximum. The average crystallite size of $CoFe_2O_4$

in $CoFe_2O_4$/MWCNTs and novel imprinted $CoFe_2O_4$/MWCNTs photocatalyst was calculated to be 12.40 nm and 13.9 nm, respectively. On the other hand, as shown in Table 1, high concentrations of Fe and Co could be detected, which further confirmed the existence of $CoFe_2O_4$. In addition, due to the coating of the surface imprinted layer, the mass percent of Fe and Co in novel imprinted $CoFe_2O_4$/MWCNTs photocatalyst was lower than that in $CoFe_2O_4$/MWCNTs.

Fig. 1 XRD patterns of $CoFe_2O_4$/MWCNTs (a) and novel imprinted $CoFe_2O_4$/MWCNTs photocatalyst (b)

Table 1 Results for the mass percent of different elements in different samples by ICP-OES

Sample	Fe (%)	Co (%)
$CoFe_2O_4$/MWCNTs	48.11	25.82
Novel imprinted $CoFe_2O_4$/MWCNTs photocatalyst	38.37	20.54

FT-IR spectra of $CoFe_2O_4$/MWCNTs and novel imprinted $CoFe_2O_4$/MWCNTs photocatalyst were shown in Fig. 2. In the spectra, the presence of peak around 582 cm^{-1} was associated with the metal-O stretching vibration.[29] It could be observed that the absorption peak at 2974 cm^{-1} attributing to the bond of C-H. Meanwhile, the absorption peaks at 1387 cm^{-1} was ascribed to the O-H bond vibration of the surface-adsorbed species of particles. The novel imprinted $CoFe_2O_4$/MWCNTs photocatalyst exhibited characteristic absorption bands near 1635 cm^{-1}, 1457 cm^{-1}, 1264 cm^{-1}, 1150 cm^{-1} and 1050 cm^{-1} which were assigned to N-H bending vibration, pyrrole ring stretch, C-N stretching and =C-H in-plane deformation, respectively.[30] Moreover, the absorption peak of 1733 cm^{-1} (-C=O group) was probably due to the existence of cross-linker or peroxidation of PPy, indicating that PPy had been formed and existed in the surface imprinted layer.[11]

Fig. 2 FT-IR spectra of $CoFe_2O_4$/MWCNTs (a) and novel imprinted $CoFe_2O_4$/MWCNTs photocatalyst (b)

TEM images of $CoFe_2O_4$/MWCNTs and novel imprinted $CoFe_2O_4$/MWCNTs photocatalyst were presented in Fig. 2. It can be clearly seen that the $CoFe_2O_4$ particles were decorated and aggregated on MWCNTs. The particle size histogram shown in Fig. 2c and 2d was obtained from many TEM images by statistical analysis method. The average particle size of $CoFe_2O_4$ particles (over 100 particles) in $CoFe_2O_4$/MWCNTs and novel imprinted $CoFe_2O_4$/MWCNTs photocatalyst were 12.03 nm and 14.12 nm, respectively. This result corresponded well with the result of XRD analysis. The specific surface areas of photocatalysts were calculated according to BET method using multi-point analysis.[31] Meanwhile, the pore volume and pore diameter were evaluated by Barrett-Joyer-Halendal (BJH) model. As shown in Table 2, compared with $CoFe_2O_4$/MWCNTs, the imprinting process of novel imprinted $CoFe_2O_4$/MWCNTs photocatalyst played an important role in creating a large number of three-dimensional imprinted cavities, thus leading to larger specific surface area.[32] The specific surface area of $CoFe_2O_4$/MWCNTs and novel imprinted $CoFe_2O_4$/MWCNTs photocatalyst was 9.627 m^2/g and 35.531 m^2/g, respectively. In addition, according to the pore size, the a-prepared novel imprinted $CoFe_2O_4$/MWCNTs photocatalyst was mesoporous.[33]

Fig. 3 TEM images of $CoFe_2O_4$/MWCNTs (a) and novel imprinted $CoFe_2O_4$/MWCNTs photocatalyst (b), particle size distribution of $CoFe_2O_4$ in $CoFe_2O_4$/MWCNTs (c) and novel imprinted $CoFe_2O_4$/MWCNTs photocatalyst (d)

Table 2 Specific surface areas and pore properties of different samples

Sample	Specific Surface Area (m^2/g)	Pore Volume (cm^3/g)	Pore Diameter (nm)
$CoFe_2O_4$/MWCNTs	9.627	0.029	9.529
Novel imprinted $CoFe_2O_4$/MWCNTs photocatalyst	35.531	0.117	3.820

Fig. 4 (left) showed the UV-vis diffuse reflectance spectra of $CoFe_2O_4$/MWCNTs and novel imprinted $CoFe_2O_4$/MWCNTs photocatalyst. It could be clearly found that both $CoFe_2O_4$/MWCNTs and novel imprinted $CoFe_2O_4$/MWCNTs photocatalyst had obvious absorption from 200 nm to 800 nm. Plots of $(Ahν)^2$ versus the energy of absorbed light afforded the band gaps of photocatalysts was shown in Fig. 4 (right). It was estimated that the bandgap of novel imprinted $CoFe_2O_4$/MWCNTs photocatalyst was 2.6 eV which was larger than that of $CoFe_2O_4$/MWCNTs, exhibiting a blue shift. The most likely reason was that the absorption band at 300 nm - 400 nm (4 eV - 3 eV) was assigned to π–π* transition of polypyrrole.[34] However, the novel imprinted $CoFe_2O_4$/MWCNTs photocatalyst could be effectively excited and generated more electron-hole pairs under the light irradiation.

Fig. 4 UV-vis DRS (left) and plots of $(Ahν)^2$ versus hν (right) for $CoFe_2O_4$/MWCNTs (a) and novel imprinted $CoFe_2O_4$/MWCNTs photocatalyst (b)

The magnetic measurement was swept from −10 kOe to 10 kOe by a vibration sample magnetometer. As shown in Fig. 5, novel imprinted $CoFe_2O_4$/MWCNTs photocatalyst showed a symmetric hysteresis curve. Indeed, the magnetization value of novel imprinted $CoFe_2O_4$/MWCNTs photocatalyst was 19 emu/g, which was much lower that of bulk $CoFe_2O_4$ (73 emu/g).[35] The decrease of saturation magnetization was due to the introduction of surface

imprinted layer. The coercivity and remanence of novel imprinted $CoFe_2O_4$/MWCNTs photocatalyst were 203.18 Oe and 5.90 emu/g, respectively, indicating that the sample was ferromagnetic.

Fig. 5 Magnetization pattern of novel imprinted $CoFe_2O_4$/MWCNTs photocatalyst at room temperature

Adsorption experiment

In order to investigate the desired time for adsorption of MBT, the adsorption experiment was carried out, and the value of adsorption capacity (Q) was shown in Fig. 6. It could be clearly seen that, before 30 min, the value of adsorption capacity increased significantly. While after 30 min, the value of adsorption capacity of novel imprinted $CoFe_2O_4$/MWCNTs photocatalyst fluctuated around 2.33 (Likewise, the value of adsorption capacity of $CoFe_2O_4$/MWCNTs fluctuated around 1.35), and the reactive process was adsorption–desorption–adsorption. Moreover, the adsorption capacity of novel imprinted $CoFe_2O_4$/MWCNTs photocatalyst was higher than that of $CoFe_2O_4$/MWCNTs, because a lot of three-dimensional imprinted cavities were existed in the surface imprinted layer, and these three-dimensional imprinted cavities had strong ability to recognize MBT. Thus, at the following experiments, 30 min was chosen as the desired time to use.

Fig. 6 The adsorption of MBT with $CoFe_2O_4$/MWCNTs (a) and novel imprinted $CoFe_2O_4$/MWCNTs photocatalyst (b)

Photocatalytic activity experiment

As we known, in this system, pyrrole was chosen as the functional monomer. Thus, different

adding concentrations of pyrrole led to different number of imprinted cavities. The photodegradation rate (Dr.) for degradation of MBT with different photocatalysts was shown in Fig. 7. As shown in Fig. 7, novel imprinted $CoFe_2O_4$/MWCNTs photocatalyst with 8 mmol pyrrole had the highest photocatalytic efficiency in 60 min under the visible light irradiation and the degradation rate (Dr.) reached 57.09 %, indicating that the suitable adding concentration of pyrrole was benefit for the preparation of novel imprinted $CoFe_2O_4$/MWCNTs photocatalyst. The lower adding concentrations, the imprinted cavities were less formed in the process of polymerization which was bad for novel imprinted $CoFe_2O_4$/MWCNTs photocatalyst. While the higher adding concentrations, the proportion of pyrrole increased, resulting in the increase of PPy, thereby, the imprinted cavities were less formed (which decreased the affinity to MBT and the photocatalytic activity of novel imprinted $CoFe_2O_4$/MWCNTs photocatalyst). At the following experiments, 8 mmol was chosen as the adding concentration of pyrrole to synthesize novel imprinted $CoFe_2O_4$/MWCNTs photocatalyst.

Fig. 7 Influence of different adding concentrations of pyrrole on the photocatalytic activity

Influence of different adding concentrations of MBT on the photocatalytic activity

Influence of different adding concentrations of MBT was investigated. As shown in Fig. 8, novel imprinted $CoFe_2O_4$/MWCNTs photocatalyst with 2 mmol MBT had the highest photocatalytic efficiency in 60 min under the visible light irradiation, indicating that the suitable adding concentration of MBT was benefit for the preparation of novel imprinted $CoFe_2O_4$/MWCNTs photocatalyst. The lower adding concentrations, the imprinted cavities were less formed in the process of polymerization which decreased the affinity to MBT and the

photocatalytic activity of novel imprinted $CoFe_2O_4$/MWCNTs photocatalyst. While the higher adding concentrations, the proportion of pyrrole decreased, resulting in the decrease of PPy, thereby, the photocatalytic activity was low. Therefore, at the following experiments, 2 mmol was chosen as the adding concentration of MBT to synthesize novel imprinted $CoFe_2O_4$/MWCNTs photocatalyst.

Fig. 8 Influence of different adding concentrations of MBT on the photocatalytic activity

The comparison of different photocatalysts

In order to investigate the photocatalytic activities of different photocatalysts, the comparative experiment was conducted. As shown in Fig. 9, after the visible light irradiation for 60 min, the degradation rate of novel imprinted $CoFe_2O_4$/MWCNTs photocatalyst reached 57.09 %, which was much higher than that of $CoFe_2O_4$/MWCNTs (22.5 %) and non-imprinted $CoFe_2O_4$/MWCNTs photocatalyst (37.29 %), because a lot of three-dimensional imprinted cavities were existed in the surface imprinted layer, and these three-dimensional imprinted cavities had strong ability to recognize and degrade MBT. Moreover, due to the fact that MWCNTs could promote the transfer of photo-generated electrons (e^-), which could further enhance the separation of e^- and photo-induced holes (h^+), thereby the degradation rate of novel imprinted $CoFe_2O_4$/MWCNTs photocatalyst was also higher than that of imprinted $CoFe_2O_4$ photocatalyst. In addition, when there was no photocatalyst in the photocatalytic system, the degradation rate was the lowest (only 7.59 %). Above result indicated that novel imprinted $CoFe_2O_4$/MWCNTs photocatalyst possessed excellent photocatalytic activity.

Fig. 9 The photocatalytic activity of different samples for photodegradation of MBT in 60 min under the visible light irradiation (a. without photocatalyst, b. $CoFe_2O_4$/MWCNTs, c. novel imprinted $CoFe_2O_4$/MWCNTs photocatalyst, d. non-imprinted $CoFe_2O_4$/MWCNTs photocatalyst, e. imprinted $CoFe_2O_4$ photocatalyst)

Selective experiment

The selective experiment was carried out by photodegrading MBT and 1-methylimidazole-2-thiol. As shown in Fig. 10, after the photodegradation of MBT in 60 min under the visible light irradiation, the photodegradation rate of novel imprinted $CoFe_2O_4$/MWCNTs photocatalyst reached 57.09 %, which was approximately 2.54 times to that of $CoFe_2O_4$/MWCNTs (22.5 %) and approximately 1.53 times to that of non-imprinted $CoFe_2O_4$/MWCNTs photocatalyst (37.29 %). Moreover, for degradation of 1-methylimidazole-2-thiol, the photodegradation rate of novel imprinted $CoFe_2O_4$/MWCNTs photocatalyst (24.23 %) was much lower than that of $CoFe_2O_4$/MWCNTs (32.11 %) and that of non-imprinted $CoFe_2O_4$/MWCNTs photocatalyst (51.63 %). These results were attributed to (i) MBT was the molecular template, which could be recognized by the three-dimensional imprinted cavities of novel imprinted $CoFe_2O_4$/MWCNTs photocatalyst. (ii) The structure of 1-methylimidazole-2-thiol was different from MBT, which could not be recognized by the imprinted cavities of novel imprinted $CoFe_2O_4$/MWCNTs photocatalyst. (iii) There was no imprinted cavities on the surface of $CoFe_2O_4$/MWCNTs and non-imprinted $CoFe_2O_4$/MWCNTs photocatalyst. Therefore, all above results demonstrated that novel imprinted $CoFe_2O_4$/MWCNTs photocatalyst not only had high photocatalytic efficiency, but also possessed the strong ability to selective photodegradation of MBT.

In addition, In order to further illustrate the selective reaction, the coefficient of selectivity was calculated, and the value of coefficient of selectivity was presented in Table 3. The coefficients of selectivity ($k_{selectivity}$) of novel imprinted $CoFe_2O_4$/MWCNTs photocatalyst relative to $CoFe_2O_4$/MWCNTs and non-imprinted $CoFe_2O_4$/MWCNTs photocatalyst was 3.37 and 3.28, respectively, indicating that $k_{selectivity}$ mainly depended on the structure of MBT, and novel imprinted $CoFe_2O_4$/MWCNTs photocatalyst possessed the three-dimensional imprinted cavities, which possessed the ability of recognizing and specifically binding MBT, the mechanism of selectivity was shown in Fig. 11. Therefore, all above results demonstrated that novel imprinted $CoFe_2O_4$/MWCNTs photocatalyst not only had high photocatalytic efficiency for photodegradation of MBT, but also possessed better selection for recognition and photodegradation of MBT.

Fig. 10 The degradation rates with $CoFe_2O_4$/MWCNTs (a, d), novel imprinted $CoFe_2O_4$/MWCNTs photocatalyst (b, e) and non-imprinted $CoFe_2O_4$/MWCNTs photocatalyst (c, f) for photodegradation of MBT (a, b, c) and 1-methylimidazole-2-thiol (d, e, f) in 60 min under the visible light irradiation

Table 3 Photodegradation rates and coefficients of selectivity with different photocatalysts in 60 min under the visible light irradiation

Photocatalyst	pollutant	Dr. (%)	$k_{imprinted}$	$k_{comparison}$	$k_{selectivity}$
$CoFe_2O_4$/MWCNTs	MBT	22.5	—	0.70	3.37
	1-methylimidazole-2-thiol	32.11			
Novel imprinted	MBT	57.09	2.36	—	—

$CoFe_2O_4$/MWCNTs	1-methylimidazole-2-thiol	24.23			
Non-imprinted	MBT	37.29	—	0.72	3.28
$CoFe_2O_4$/MWCNTs	1-methylimidazole-2-thiol	51.63			

Fig. 11 The mechanism of selectivity

Photocatalytic mechanism

In order to investigate the photocatalytic mechanism of degradation of MBT with novel imprinted $CoFe_2O_4$/MWCNTs photocatalyst, the corresponding experiments were carried out in accordance with the photocatalytic activity experiment in Experimental section, but at the beginning of the photocatalytic reaction, some quenchers were added into the MBT aqueous solution, such as triethanolamine (TEOA), tert-butyl alcohol (tBuOH) or nitrogen (N_2). During the photocatalytic process, TEOA (0.1 mmol), tBuOH (0.1 mmol) and N_2 (kept the N_2 atmosphere) acted as the quenchers for h^+, $\bullet OH$, and $\bullet O_2^-$, respectively. The photodegradation rates in presence of different quenchers were shown in Fig. 12. It could be clearly seen that the addition of TEOA and tBuOH both had significant effect on the photocatalytic activity, while the addition of N_2 had little effect on the photocatalytic activity. Therefore, in the process of photodegradation reaction, h^+ and $\bullet OH$ were the main oxidative species, $\bullet O_2^-$ played a very small role.

Fig. 12 The photodegradation rates of novel imprinted $CoFe_2O_4$/MWCNTs photocatalyst for degradation of MBT in presence of different quenchers in 60 min under the visible light irradiation

According to above results, the possible photocatalytic mechanism was presented, which was shown in Fig. 13. When novel imprinted $CoFe_2O_4$/MWCNTs photocatalyst was irradiated by the

visible light, the photo-generated electrons (e^-) and photo-induced holes (h^+) were generated in PPy and $CoFe_2O_4$. Afterwards, e^- in PPy transferred into $CoFe_2O_4$, then the e^- in $CoFe_2O_4$ further transferred into MWCNTs, meanwhile h^+ left in $CoFe_2O_4$ transferred into PPy. Therefore, more and more e^-/h^+ formed and triggered the formation of very reactive radicals super-oxide radical ion ($O_2^{\cdot -}$) and hydroxyl radical ($\cdot OH$), which were responsible for the photodegradation of MBT. The detailed reaction steps of the whole process were described as follows:

$$\text{Novel imprinted } CoFe_2O_4 \text{ / MWCNTs photocatalyst} + hv \rightarrow \text{PPy}(h^+ + e^-) + CoFe_2O_4(h^+ + e^-) \quad (5)$$

$$\text{PPy}(e^-) \xrightarrow{\text{transfer}} CoFe_2O_4 \xrightarrow{\text{further transfer}} \text{MWCNTs} \quad (6)$$

$$CoFe_2O_4(h^+) \xrightarrow{\text{transfer}} \text{PPy} \quad (7)$$

$$\text{PPy}(h^+) + \text{MBT} \rightarrow CO_2 + H_2O + \text{other small molecules (major)} \quad (8)$$

$$\text{PPy}(h^+) + H_2O/OH^- \rightarrow \bullet OH \quad (9)$$

$$CoFe_2O_4(e^-) + O_2 \rightarrow \bullet O_2^- \quad (10)$$

$$\bullet O_2^- + \text{MBT} \rightarrow CO_2 + H_2O + \text{other small molecules (minor)} \quad (11)$$

$$\bullet O_2^- + H^+ \rightarrow \bullet OH \quad (12)$$

$$\bullet OH + \text{MBT} \rightarrow CO_2 + H_2O + \text{other small molecules (major)} \quad (13)$$

Fig. 13 Photocatalytic mechanism of novel imprinted $CoFe_2O_4$/MWCNTs photocatalyst

Reproducibility of novel imprinted $CoFe_2O_4$/MWCNTs photocatalyst

In order to evaluate the photochemical stability of novel imprinted $CoFe_2O_4$/MWCNTs photocatalyst for photodegradation of MBT, the experiment of Reproducibility was conducted. As shown in Fig. 14, the novel imprinted $CoFe_2O_4$/MWCNTs photocatalyst was reusable and maintain relatively high activity after five consecutive cycles, indicating that the as-prepared novel

imprinted $CoFe_2O_4$/MWCNTs photocatalyst had excellent photochemical stability. The decreased photocatalytic activity was probably caused by slight aggregation of nanoparticles during the photocatalytic process[36] and accumulation of organic intermediates in the cavities and on the surface of the photocatalyst affecting the adsorption of MBT.[37]

Fig. 14 Reproducibility of novel imprinted $CoFe_2O_4$/MWCNTs photocatalyst for photodegradation of MBT in 60 min under the visible light irradiation

Conclusions

In summary, based on MBT as the molecular template, pyrrole as the imprinted functional monomer and conductive polymerizable monomer, $CoFe_2O_4$/MWCNTs as the matrix material, novel imprinted $CoFe_2O_4$/MWCNTs photocatalyst was prepared through combination of hydrothermal method and suspension polymerization. The results indicated that the surface imprinted layer was successfully coated on the surface of $CoFe_2O_4$/MWCNTs and PPy was formed and existed in the surface imprinted layer, the magnetic saturation value of novel imprinted $CoFe_2O_4$/MWCNTs photocatalyst was 19 emu/g. Moreover, compared with other photocatalysts, novel imprinted $CoFe_2O_4$/MWCNTs photocatalyst not only had high photocatalytic efficiency, the degradation rate reached 57.09 %, but also possessed the strong ability to selective recognition and photodegradation of MBT, the coefficients of selectivity of novel imprinted $CoFe_2O_4$/MWCNTs photocatalyst relative to $CoFe_2O_4$/MWCNTs and non-imprinted $CoFe_2O_4$/MWCNTs photocatalyst was 3.37 and 3.28, respectively. In addition, in the process of photodegradation reaction, h^+ and $\bullet OH$ were the main oxidative species, $\bullet O_2^-$

played a very small role.

Acknowledgments

This work was financially supported by the National Natural Science Foundation of China (No. 21306068), the Natural Science Foundation of Jiangsu Province (Nos. BK20130477, BK20130487 and BK20140532), the China Postdoctoral Science Foundation (Nos. 2012M521015 and 2014T70486), the Innovation Programs Foundation of Jiangsu Province (Nos. CXZZ13_0693) and the University Professional Degree Postgraduate Research Practice Program of Jiangsu Province (No. 1011310016).

References

1 F. B. Li, X. Z. Li, M. F. Hou, K. W. Cheah and W. C. H. Choy, *Appl. Catal., A*, 2005, **285**, 181.

2 F. B. Li, X. Z. Li and K. H. Ng, *Ind. Eng. Chem. Res.*, 2006, **45**, 1.

3 M. H. Habibi, S. Tangestaninejad and B. Yadollahi, *Appl. Catal., B*, 2001, **33**, 57.

4 C. S. Liu, F. B. Li, X. M. Li, G. Zhang and Y. Q. Kuang, *J. Mol. Catal., A*, 2006, **252**, 40.

5 Z.Y. Lu, W.Z. Zhou, P.W. Huo, Y.Y. Luo, M. He, J.M. Pan, C.X. Li and Y.S. Yan, *Chem. Eng. J.*, 2013, **217**, 398.

6 M. Pelaez, P. Falaras, A.G. Kontos, A.A. de la Cruz, K. O'shea, P.S.M. Dunlop, J.A. Byrne and D.D. Dionysiou, *Appl. Catal., B*, 2012, **121–122**, 30.

7 Z.Y. Cai, Z.G. Xiong, X.M. Lu and J.H. Teng, *J. Mater. Chem. A*, 2014, **2**, 545.

8 D. F. Zhang, X. P. Pu, Y. Y. Gao, C. H. Su, H. Li, H. Y. Li and W. X. Hang, *Mater. Lett.*, 2013, **113**, 179.

9 C. J. Li, J. N. Wang, B. Wang, J. R. Gong and Z. Lin, *Mater. Res. Bull.*, 2012, **47**, 333.

10 P. Sathishkumar, R. V. Mangalaraja, S. Anandan and M. Ashokkumar, *Chem. Eng. J.*, 2013, **220**, 302.

11 Z. R. Zhu, X. Y. Li, Q. D. Zhao, Y. Shi, H. Li and G. H. Chen, *J. Nanopart. Res.*,2011, **13**, 2147.

12 A. A. Farghali, M. Bahgat, W.M.A. El Rouby, M. H. Khedr, *J. Solution Chem.*, 2012, **41**, 2209.

13 A. A. Farghali, M. Bahgat, W.M.A. El Rouby, M. H. Khedr, *J. Nanostruct. Chem.*, 2013, **3**, 1.

14 Y.Y. Luo, Z.Y. Lu, Y.H. Jiang, D.D. Wang, L.L. Yang, P.W. Huo, Z.L. Da, X.L. Bai, X.L. Xie and P.Y. Yang, *Chem. Eng. J.*, 2014, **240**, 244.

15 J. H. Sui, C. Zhang, J. Li, Z. L. Yu and W. Cai, *Mater. Lett.*, 2012, **75**, 158.

16 B. Unal, M. Senel, A. Baykal and H. Sözeri, *Curr. Appl. Phys.*, 2013, **13**, 1404.

17 Z.Y. Lu, F. Chen, M. He, M.S. Song, Z.F. Ma, W.D. Shi, Y.S. Yan, J.Z. Lan, F. Li and P. Xiao, *Chem. Eng. J.*, 2014, **249**, 15.

18 H.C. Liu and W. Chen, *RSC Adv.*, 2015, **5**, 27034.

19 G.F. Zhu, J. Fan, Y.B. Gao, X. Gao and J.J. Wang, *Talanta*, 2011, **84**, 1124.

20 A. Menaker, V. Syritski, J. Reut, A. Öpik, V. Horváth and R.E. Gyurcsányi, *Adv. Mater.*, 2009, **21**, 2271.

21 L.C. Xu, J.M. Pan, J.D. Dai, Z.J. Cao, H. Hang, X.X. Li and Y.S. Yan, *RSC Adv.*, 2012, **2**, 5571.

22 D. Sharabi and Y. Paz, *Appl. Catal., B*, 2010, **95**, 169.

23 Z.Y. Lu, P.W. Huo, Y.Y. Luo, X.L. Liu, D. Wu, X. Gao, C.X. Li and Y.S. Yan, *J. Mol. Catal., A*, 2013, **378**, 91.

24 Z.Y. Lu, Y.Y. Luo, M. He, P.W. Huo, T.T. Chen, W.D. Shi, Y.S. Yan, J.M. Pan, Z.F. Ma and S.Y. Yang, *RSC Adv.*, 2013, **3**, 18373.

25 J. J. Li, J. T. Feng and W. Yan, *Appl. Surf. Sci.*, 2013, **279**, 400.

26 H. Khan, T. Khan and J. K. Park, *Sep. Purif. Technol.*, 2008, **62**, 363.

27 C. H. Chen, Y. H. Liang and W. D. Zhang, *J. Alloy. Compd.*, 2010, **501**, 168.

28 H. A. J. L. Mourão, A. R. Malagutti and C. Ribeiro, *Appl. Catal., A*, 2010, **382**, 284.

29 Y. Wang, J. Park, B. Sun, H. Ahn and G. X. Wang, *Chem. Asian J.*, 2012, **7**, 1940.

30 S. Gu, B. Li, C. J. Zhao, Y. L. Xu, X. Z. Qian and G. R. Chen, *J. Alloys Compd.*, 2011, **509**, 5677.

31 M. Tada, T. Sasaki and Y. Iwasawa, *J. Catal.*, 2002, **211**, 496.

32 W. Kareuhanon, V. S. Lee, P. Nimmanpipug, C. Tayapiwatana and M. Pattarawarapan, *Chromatographia*, 2009, **70**, 1531.

33 W. M. Yang, L. K. Liu, Z. P. Zhou, H. Liu, B. Z. Xie and W. Z. Xu, *Appl. Surf. Sci.*, 2013, **282**, 809.

34 K. Dutta and S. K. De, *Solid State Commun.*, 2006, **140**, 167.

35 M. Abbas, B. P. Rao, M. N. Islam, K. W. Kim, S. M. Naga, M. Takahashi and C. Kim, *Ceram. Int.*, 2014, **40**, 3269.

36 F. Wang, S. X. Min, Y. Q. Han and L. Feng, *Superlattice. Microst.*, 2010, **48**, 170.

37 S. Gomez, C. L. Marchena, L. Pizzio and L. Pierella, *J. Hazard. Mater.*, 2013, **258**–**259**, 19.

Figures

Fig. 1 XRD patterns of $CoFe_2O_4$/MWCNTs (a) and novel imprinted $CoFe_2O_4$/MWCNTs photocatalyst (b)

Fig. 2 FT-IR spectra of $CoFe_2O_4$/MWCNTs (a) and novel imprinted $CoFe_2O_4$/MWCNTs photocatalyst (b)

Fig. 3 TEM images of $CoFe_2O_4$/MWCNTs (a) and novel imprinted $CoFe_2O_4$/MWCNTs photocatalyst (b), particle size distribution of $CoFe_2O_4$ in $CoFe_2O_4$/MWCNTs (c) and novel imprinted $CoFe_2O_4$/MWCNTs photocatalyst (d)

Fig. 4 UV-vis DRS (left) and plots of $(Ahv)^2$ versus hv (right) for $CoFe_2O_4$/MWCNTs (a) and novel imprinted $CoFe_2O_4$/MWCNTs photocatalyst (b)

Fig. 5 Magnetization pattern of novel imprinted $CoFe_2O_4$/MWCNTs photocatalyst at room temperature

Fig. 6 The adsorption of MBT with $CoFe_2O_4$/MWCNTs (a) and novel imprinted $CoFe_2O_4$/MWCNTs photocatalyst (b)

Fig. 7 Influence of different adding concentrations of pyrrole on the photocatalytic activity

Fig. 8 Influence of different adding concentrations of MBT on the photocatalytic activity

Fig. 9 The photocatalytic activity of different samples for photodegradation of MBT in 60 min under the visible light irradiation (a. without photocatalyst, b. $CoFe_2O_4$/MWCNTs, c. novel imprinted $CoFe_2O_4$/MWCNTs photocatalyst, d. non-imprinted $CoFe_2O_4$/MWCNTs photocatalyst, e. imprinted $CoFe_2O_4$ photocatalyst)

Fig. 10 The degradation rates with $CoFe_2O_4$/MWCNTs (a, d), novel imprinted $CoFe_2O_4$/MWCNTs

photocatalyst (b, e) and non-imprinted $CoFe_2O_4$/MWCNTs photocatalyst (c, f) for photodegradation of MBT (a, b, c) and 1-methylimidazole-2-thiol (d, e, f) in 60 min under the visible light irradiation

Fig. 11 The mechanism of selectivity

Fig. 12 The photodegradation rates of novel imprinted $CoFe_2O_4$/MWCNTs photocatalyst for degradation of MBT in presence of different quenchers in 60 min under the visible light irradiation

Fig. 13 Photocatalytic mechanism of novel imprinted $CoFe_2O_4$/MWCNTs photocatalyst

Fig. 14 Reproducibility of novel imprinted $CoFe_2O_4$/MWCNTs photocatalyst for photodegradation of MBT in 60 min under the visible light irradiation

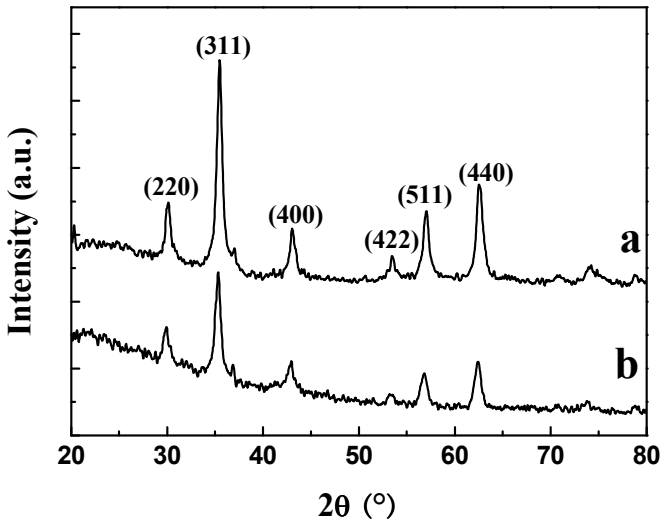

Fig. 1 XRD patterns of $CoFe_2O_4$/MWCNTs (a) and novel imprinted $CoFe_2O_4$/MWCNTs photocatalyst (b)

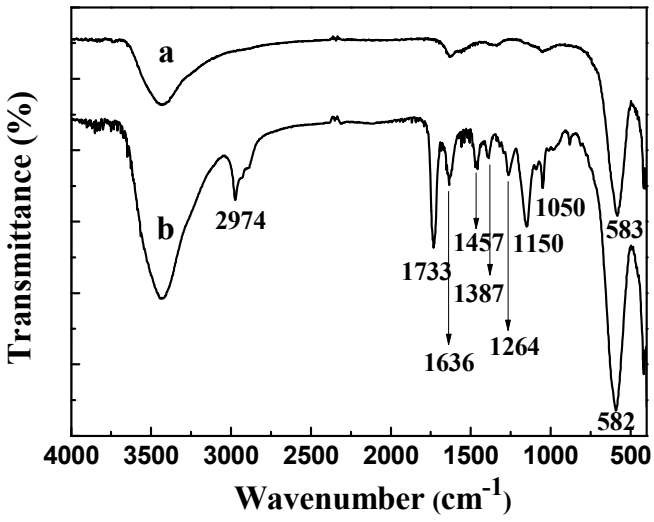

Fig. 2 FT-IR spectra of $CoFe_2O_4$/MWCNTs (a) and novel imprinted $CoFe_2O_4$/MWCNTs photocatalyst (b)

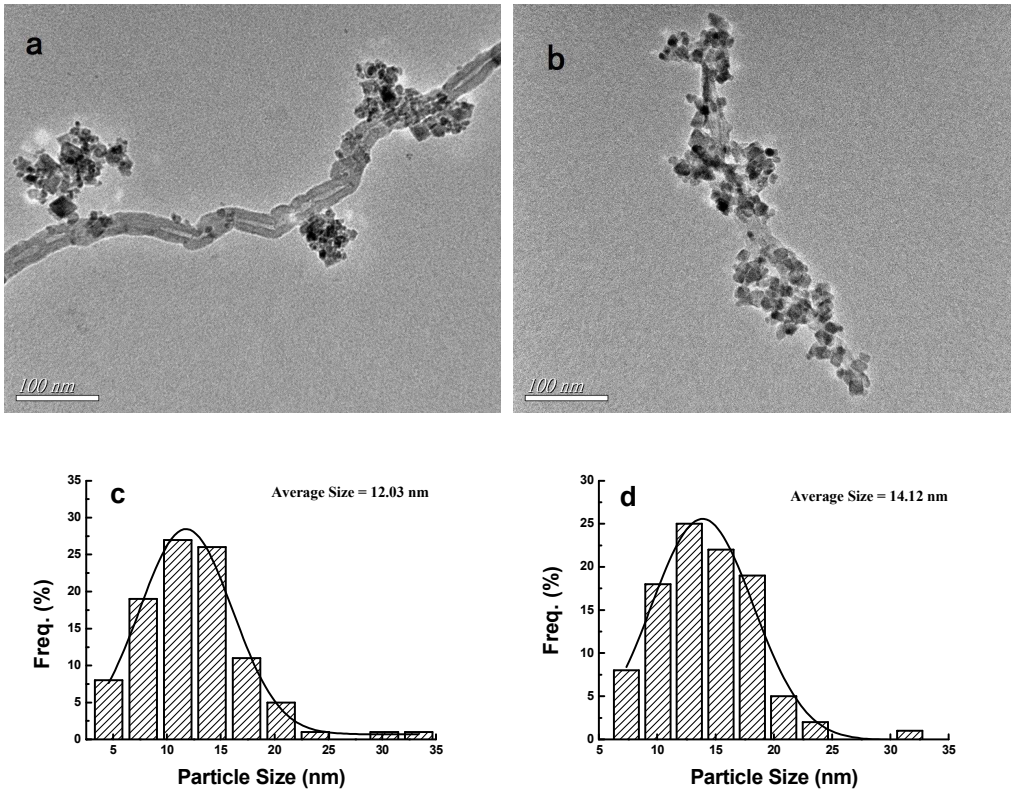

Fig. 3 TEM images of $CoFe_2O_4$/MWCNTs (a) and novel imprinted $CoFe_2O_4$/MWCNTs photocatalyst (b), particle size distribution of $CoFe_2O_4$ in $CoFe_2O_4$/MWCNTs (c) and novel imprinted $CoFe_2O_4$/MWCNTs photocatalyst (d)

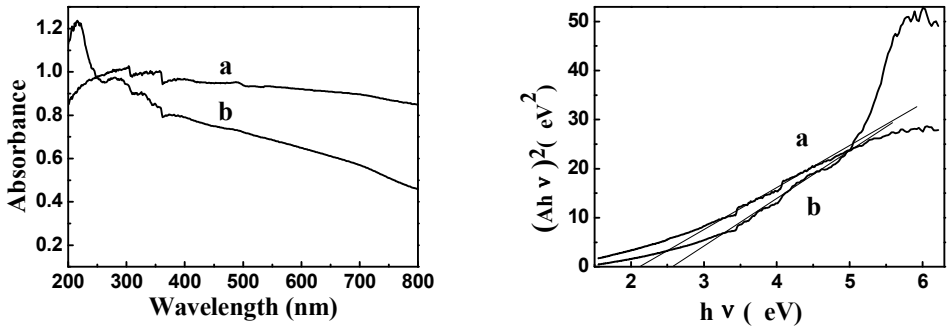

Fig. 4 UV-vis DRS (left) and plots of $(Ahv)^2$ versus hν (right) for $CoFe_2O_4$/MWCNTs (a) and novel imprinted $CoFe_2O_4$/MWCNTs photocatalyst (b)

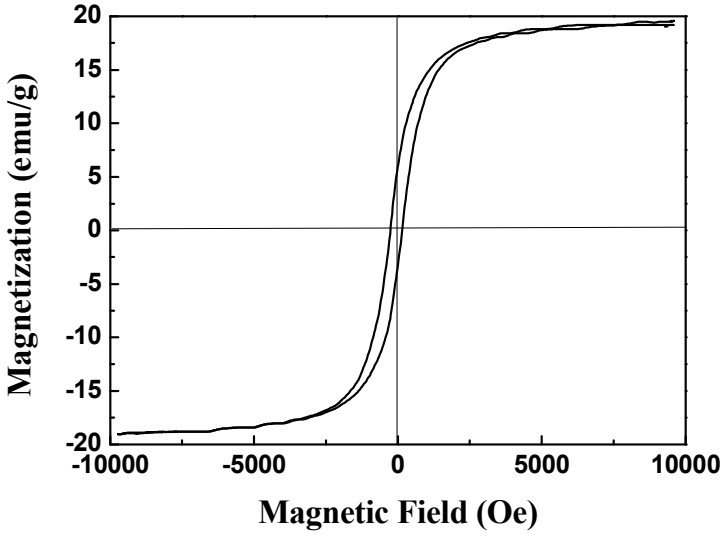

Fig. 5 Magnetization pattern of novel imprinted $CoFe_2O_4$/MWCNTs photocatalyst at room temperature

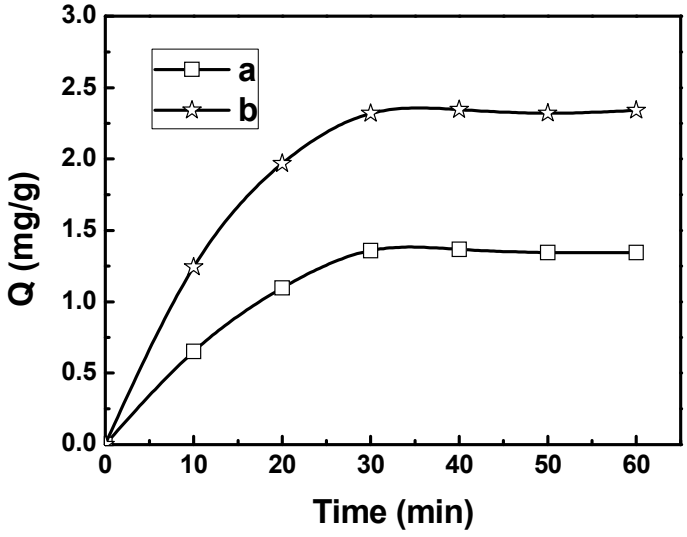

Fig. 6 The adsorption of MBT with $CoFe_2O_4$/MWCNTs (a) and novel imprinted $CoFe_2O_4$/MWCNTs photocatalyst (b)

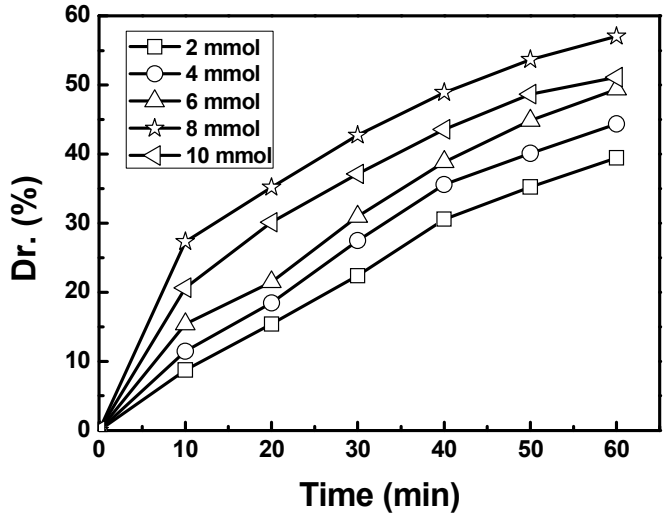

Fig. 7 Influence of different adding concentrations of pyrrole on the photocatalytic activity

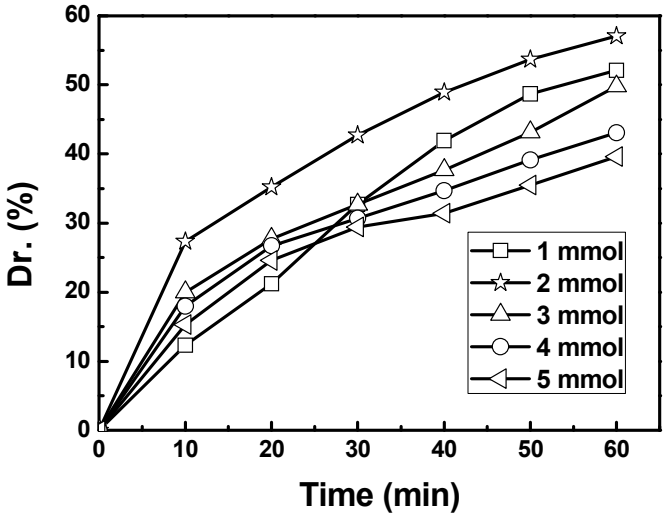

Fig. 8 Influence of different adding concentrations of MBT on the photocatalytic activity

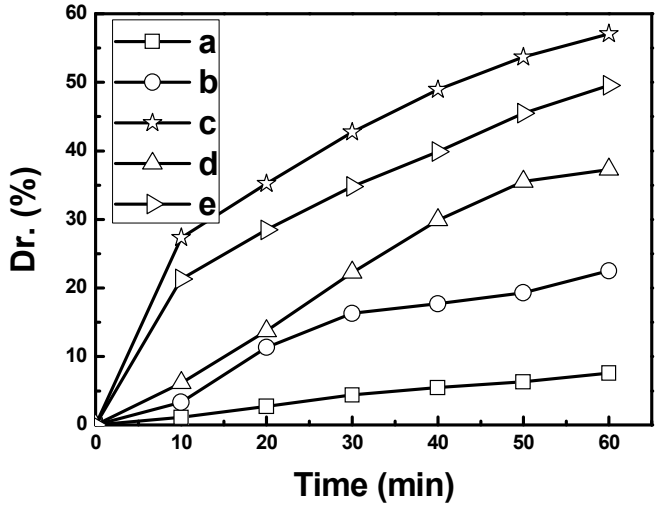

Fig. 9 The photocatalytic activity of different samples for photodegradation of MBT in 60 min under the visible light irradiation (a. without photocatalyst, b. $CoFe_2O_4$/MWCNTs, c. novel imprinted $CoFe_2O_4$/MWCNTs photocatalyst, d. non-imprinted $CoFe_2O_4$/MWCNTs photocatalyst, e. imprinted $CoFe_2O_4$ photocatalyst)

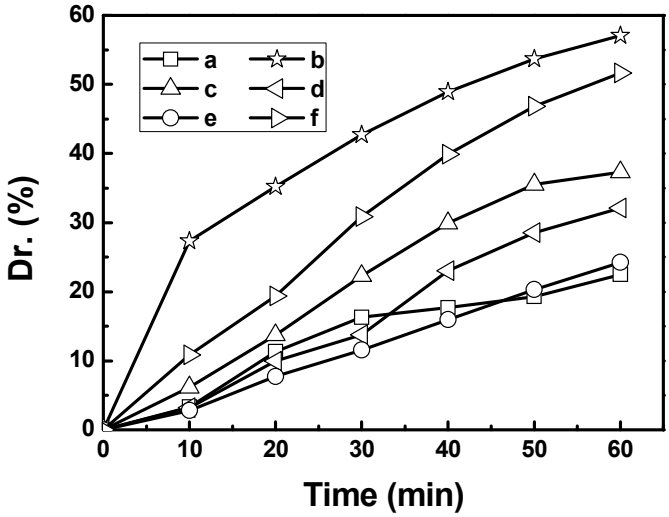

Fig. 10 The degradation rates with $CoFe_2O_4$/MWCNTs (a, d), novel imprinted $CoFe_2O_4$/MWCNTs photocatalyst (b, e) and non-imprinted $CoFe_2O_4$/MWCNTs photocatalyst (c, f)

for photodegradation of MBT (a, b, c) and 1-methylimidazole-2-thiol (d, e, f) in 60 min under the visible light irradiation

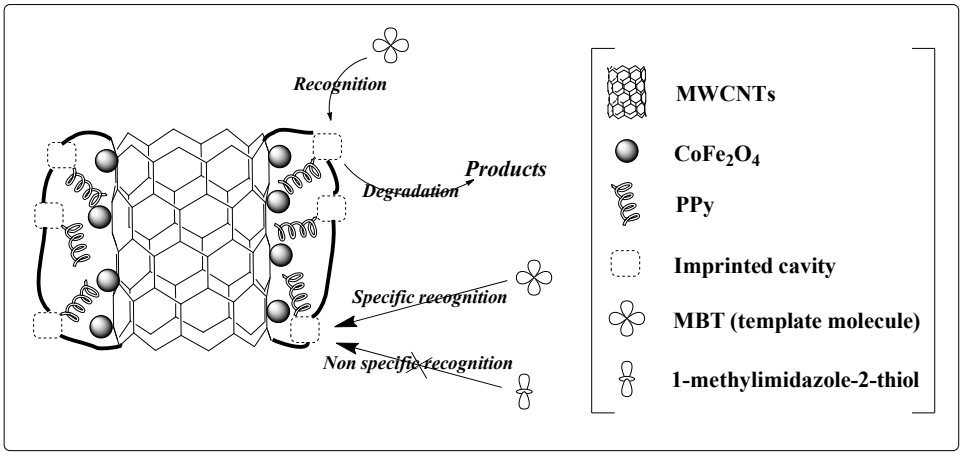

Fig. 11 The mechanism of selectivity

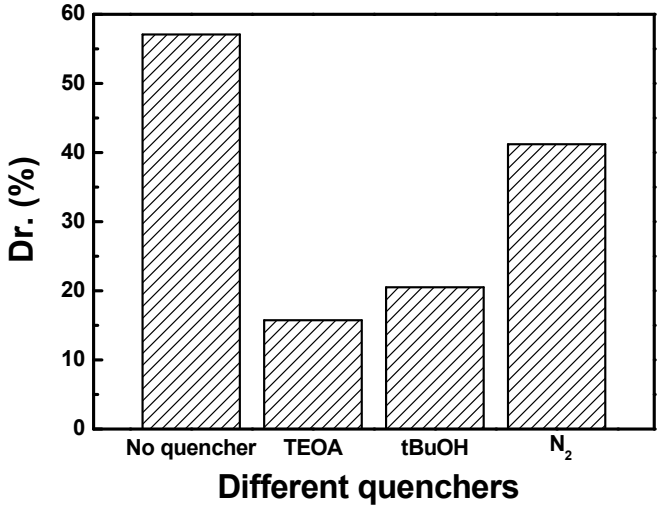

Fig. 12 The photodegradation rates of novel imprinted $CoFe_2O_4$/MWCNTs photocatalyst for degradation of MBT in presence of different quenchers in 60 min under the visible light irradiation

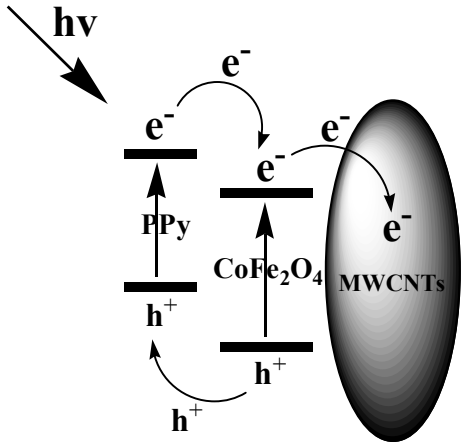

Fig. 13 Photocatalytic mechanism of novel imprinted $CoFe_2O_4$/MWCNTs photocatalyst

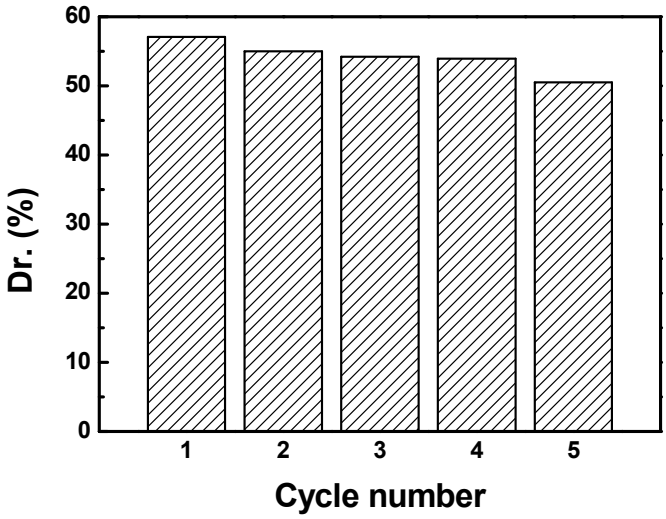

Fig. 14 Reproducibility of novel imprinted $CoFe_2O_4$/MWCNTs photocatalyst for photodegradation of MBT in 60 min under the visible light irradiation